



# Observation of large wave vector interface spin waves: Ni(100)/fcc Co(100) and Cu(100)/Co(100)

J. Rajeswari,<sup>1,2</sup> H. Ibach,<sup>3,2,\*</sup> and C. M. Schneider<sup>1,2</sup>

<sup>1</sup>*Peter Grünberg Institut (PGI-6), Forschungszentrum Jülich, 52425 Jülich, Germany*

<sup>2</sup>*Jülich Aachen Research Alliance, Germany*

<sup>3</sup>*Peter Grünberg Institut (PGI-3), Forschungszentrum Jülich, 52425 Jülich, Germany*

(Received 19 February 2013; published 14 June 2013)

Using electron energy loss spectroscopy, we have probed the spin waves of fcc(100) cobalt after capping with 1–3 atom layers of pseudomorphic nickel or up to 12 atom layers of copper. The intensity decay of the spin wave signal is quantitatively described by the mean-free path of the incident and the scattered electron within the capping layer. The observed spin waves are therefore localized at the cobalt side of the Co/Ni and Co/Cu interfaces. Compared to the free cobalt surface, the interface spin waves are downshifted in frequency. The effect is attributed to a reduced exchange interaction between cobalt atoms at the interface.

DOI: [10.1103/PhysRevB.87.235415](https://doi.org/10.1103/PhysRevB.87.235415)

PACS number(s): 75.30.Ds, 75.70.Cn

Wave packets of spin waves offer the unique capability to transport a quantum bit, the spin, without the transport of charge or mass. In this context, large wave vector/high-energy spin waves are of particular interest as they permit a spin confinement within a few nanometers.<sup>1,2</sup> Stimulated by the development of advanced electron energy loss spectrometers,<sup>3,4</sup> a considerable number of experimental studies concerning large wave vector/high-energy surface spin waves of 3*d* metal films have emerged lately.<sup>5–12</sup> These studies were accompanied, partly even anticipated, by considerable efforts in theory aiming at the understanding of localized spin waves in thin films of itinerant magnets and at the description of inelastic electron scattering from such excitations.<sup>13–25</sup> In accordance with the surface sensitivity of low-energy electron spectroscopy, experimental studies focused on spin waves localized at surfaces and on spin waves in 1–2 monolayer (ML) thick films. In view of the importance of interfaces between magnetic materials as well as between magnetic and nonmagnetic materials for giant magnetoresistance (GMR) and spin valve devices, experimental means to characterize spin waves localized at *interfaces* would be highly desirable. Some indirect information on the spin waves localized at an interface may be obtained from the recently observed lowest-energy standing spin wave mode of a cobalt film<sup>26</sup> since this mode corresponds to the antisymmetric combination of the two surface modes at either surface of the film. A direct experimental access to the spin waves localized at interfaces, however, was not available up to now.

In this paper, we show that low-energy inelastic electron scattering can be employed to directly probe spin waves at metal/metal interfaces. We exploit the fact that electrons of very low energy have a mean-free path, which is large enough to penetrate a thin capping layer deposited onto a magnetic film. This permits a unique experimental access to the spin waves localized at the interface between the magnetic thin film and the capping layer.

The specific system that we have investigated is the surface of an 8-ML fcc cobalt film grown on Cu(100),<sup>5,26</sup> upon which we grow epitaxial capping layers of varying thickness. As capping materials we have chosen nickel and copper: we have selected nickel, since one might envision that cobalt induces a higher magnetic moment to the nickel atoms at the interface

via some proximity effect<sup>27</sup> so that the surface spin waves of cobalt would extend into the nickel overlayer. This would be particularly interesting since all attempts to observe the large wave vector surface spin waves on pure nickel have failed so far.<sup>28</sup> As second capping material, we selected copper since we anticipated the observation of interface spin waves through thicker layers of copper due to the larger mean-free path. We find that for both capping materials the intensities and the peak energies of the spin wave signals drop down upon deposition of 1–3 layers. Beyond the initial drop, the spin wave energies stay constant while the intensities decay exponentially with coverage. The exponential decay is well described by a mean-free-path model, which considers the electron/spin wave interaction to take place at the cobalt side of the interface.

The Cu(100) templates are prepared by repeated cycles of sputtering with 1-keV argon atoms followed by annealing to 450°C. Cobalt, nickel, and copper are deposited using electron beam stimulated evaporation from rods. The thicknesses of the deposited layers are calibrated by the intensity oscillations of the specular reflection of 3-keV electrons at grazing incidence, caused by the roughness oscillations during the pseudomorphic growth of Ni and Cu on the fcc Co(100) films (see, e.g., Chap. 11 of Ref. 29). Electron energy loss spectra of the spin waves are obtained by employing a specially designed spectrometer.<sup>4,30</sup> The high stability of the spectrometer (equipped with a conventional LaB<sub>6</sub> cathode) ensures the reproducibility of intensities within a few percent. The differences in the intensities of spin wave spectra of samples prepared on different days are smaller than 8%. All spin wave spectra were recorded with a scattering angle of 90°. The momentum transfer parallel to the surface  $\Delta K_{\parallel}$  is adjusted by rotation of the sample manipulator.

Figure 1 shows a series of spin wave spectra after deposition of Ni on an 8-ML film of fcc cobalt on Cu(100). The impact energy is chosen as  $E_0 = 6$  eV since the spin wave intensity has a maximum around this impact energy. The angle of incidence is  $\theta^{(i)} = 21.8^\circ$  and the exit angle therefore  $\theta^{(s)} = 90^\circ - 21.8^\circ = 68.2^\circ$ . The wave vector transfer to the surface is calculated from wave vector conservation

$$\Delta K_{\parallel} = k^{(s)} \sin \theta^{(s)} - k^{(i)} \sin \theta^{(i)} = -q_{\parallel} \quad (1)$$

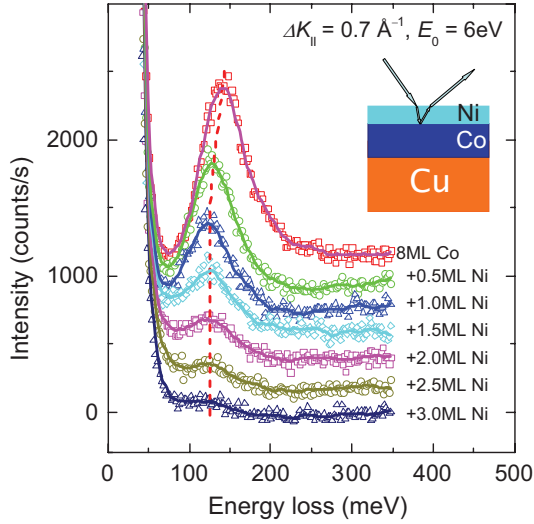


FIG. 1. (Color online) A series of spectra for the bare 8-ML Co film deposited on Cu(100) and for the cobalt film covered with additional 0.5–3 ML Ni (from top to bottom). The spectra are vertically shifted with respect to each other. The solid lines are an 11-point gliding average to guide the eye. The dashed line connects the peak maxima. The inset illustrates the electron path (see text).

in which  $k^{(s)}$  and  $k^{(i)}$  denote the modulus of the wave vector of the scattered and incident electrons, respectively, and  $q_{||}$  is the wave vector of the spin wave. The wave vector transfer is along the  $(110)$  ( $\bar{\Gamma}\bar{X}$ ) direction. For small energy losses ( $k^{(s)} = k^{(i)}$ ),  $\Delta K_{||}$  is  $0.7 \text{ \AA}^{-1}$ .  $\Delta K_{||}$  reduces slightly with increasing energy loss and amounts to  $0.686 \text{ \AA}^{-1}$  for an energy loss of 140 meV. The upper spectrum in Fig. 1 is for the bare surface of the 8-ML cobalt film. The loss peak centered at about 140 meV represents the excitation of the surface spin wave of the fcc cobalt film. The energy is in agreement with the previous studies,<sup>5,26,31</sup> We remark that for  $\Delta K_{||} = 0.7 \text{ \AA}^{-1}$  the spin wave amplitude decays exponentially in deeper Co layers with a decay length equivalent to about 2 ML. Hence, there is no influence of the Cu(100) substrate crystal on the spin waves except that the epitaxial relationship between the substrate and the Co film stabilizes the fcc structure of cobalt. Upon deposition of nickel, the spin wave energy shifts downwards and levels off at  $\approx 125 \text{ meV}$  for coverages beyond 1 ML. The intensity of the spin wave peak drops continuously with increasing thickness of the Ni film. For an accurate comparison of the intensities, we fit a Gaussian to the spin wave signal (see Ref. 26 for details). Since the spin wave peak is a factor of 2 broader than the elastic peak, the count rate in the spin wave loss is roughly proportional to the full width at half maximum (FWHM) of the elastic peak. We therefore take the count rate in the maximum of the Gaussian divided by the FWHM of the elastic peak as a measure of the intensity of the spin wave excitation (*specific intensity*  $I_{\text{specific}}$ ). Specific intensities  $I_{\text{specific}}$  and peak energies of the spin wave losses are plotted in Fig. 2 as a function of nickel coverage by open and solid symbols, respectively. Squares and triangles represent the results of independently prepared surfaces. The open circles mark the specific intensity for the case where angle of incidence and angle of the emerging beam are

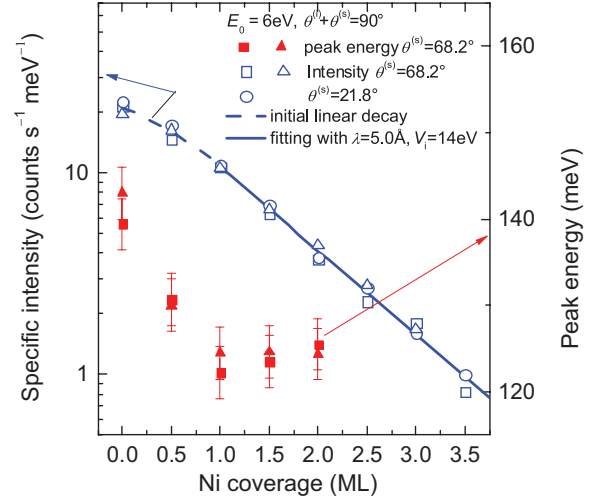


FIG. 2. (Color online) Specific intensity and peak energy of the spin wave energy loss at  $\Delta K_{||} = 0.7 \text{ \AA}^{-1}$  vs coverage with nickel. The energy shifts downwards until a monolayer is completed and stays constant thereafter. The exponential decay of the intensity for thicker layers is quantitatively described by the path length of electrons inside the nickel layer showing that the electron/spin wave interaction occurs at the Co/Ni interface.

inverted ( $\theta^{(i)} = 68.2^\circ$  and  $\theta^{(s)} = 21.8^\circ$  instead of  $\theta^{(i)} = 21.8^\circ$  and  $\theta^{(s)} = 68.2^\circ$ ) which flips the wave vector from  $+0.7 \text{ \AA}^{-1}$  to  $-0.7 \text{ \AA}^{-1}$ , respectively. The specific intensity is the same for both cases within the limits of error. The dashed and solid lines describe the specific intensity by a linear decrease below 1-ML coverage and by an exponential decrease beyond 1 ML, respectively.

The exponential decay of the specific intensity beyond 1-ML coverage points toward a spin wave excitation localized at the Co/Ni interface. The intensity should decay exponentially in that case as electrons must first traverse the Ni layer without energy loss on their way to the interface and second on their way out after interaction with the spin wave at the interface. In the following, we show that the observed decay can be quantitatively described by the mean-free path of electrons in nickel. The specific intensity as a function of the number of deposited layers  $N$  is

$$I_{\text{specific}}(N) = I_0 \exp[-\Lambda(N)/\lambda] \quad (2)$$

with  $\Lambda(N)$  the path length inside the Ni layer and  $\lambda$  the mean-free path. For the moment,  $N$  is treated as a continuous variable. The path length  $\Lambda(N)$  is

$$\Lambda(N) = (a_0/2)N \left[ 1/\cos(\theta_{(\text{inside})}^{(i)}) + 1/\cos(\theta_{(\text{inside})}^{(s)}) \right] \quad (3)$$

in which  $a_0$  is the lattice constant of Ni and  $\theta_{(\text{inside})}^{(i)}$  and  $\theta_{(\text{inside})}^{(s)}$  are the angles of incident and scattered electrons inside the Ni layer, respectively. These angles are smaller than the angles outside because of the larger kinetic energy inside the solid and the resulting refraction of the electron waves at the surface (inset Fig. 1). The relation between the polar angle inside and outside is

$$\theta_{(\text{inside})}^{(i,s)} = \arctan \left[ \frac{\sin \theta^{(i,s)}}{\cos \theta^{(i,s)} \sqrt{\frac{E_0}{E_0 + V_i}}} \right]. \quad (4)$$

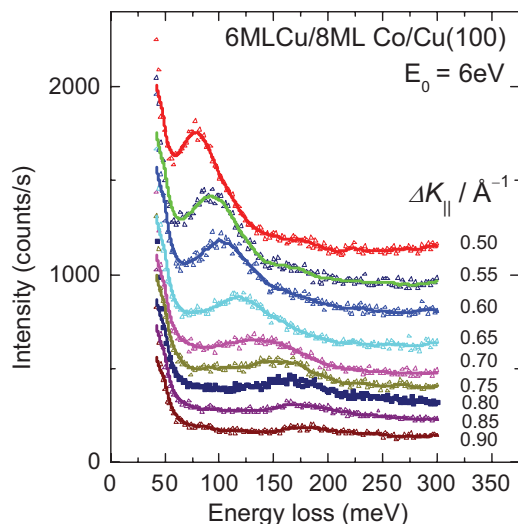


FIG. 3. (Color online) Series of spin wave spectra of the 6 ML Cu/8 ML Co/Cu(100) system as function of wave vector  $\Delta K_{\parallel}$ . Spectra are shifted with respect to each other along the vertical axis.

Here,  $V_i$  is the inner potential of the Ni layer. The mean-free path  $\lambda$  of electrons in nickel has been calculated by Hong and Mills.<sup>32</sup> For the energy of  $E_0 = 6$  eV relative to the vacuum level (approximately 11 eV relative to the Fermi level) the authors found the mean-free path to be  $\lambda = 5$  Å, practically independent of energy. With that number and the absolute value of the specific intensity fitted to 1-ML coverage, the solid line in Fig. 2 is obtained for  $V_i = 14$  eV. The assumption of 14 eV is not critical. Assuming, e.g.,  $V_i = 10$  eV would result in only a 5% increase of the path length.

The model assumes a continuous growth of the thickness of the Ni layer. In order to check for the influence of discreteness of the layers, we have simulated the growth of Ni layers with various ratios of the hopping rate for single atoms  $\nu$  and the surface atom-specific flux  $F$  to obtain either nearly perfect layer-by-layer growth ( $\nu/F = 20000$ ) or a rather rough surface with nearly a Poisson distribution of open layers ( $\nu/F = 10$ ).<sup>29</sup> We have then calculated the intensities by averaging the area-weighted intensities obtained for different local thicknesses of the Ni layer. The differences between the continuum model and the discrete model are rather small. They amount to a difference in the mean-free path  $\lambda = 5.1$  Å instead of  $\lambda = 5.0$  Å for  $\nu/F = 20000$  and  $\lambda = 5.2$  Å instead of  $\lambda = 5.0$  Å for  $\nu/F = 10$ .

The good agreement of the mean-free-path model and the experimental intensities demonstrates that the electrons lose the characteristic spin wave energy at the cobalt side of the Ni/Co interface. The observed spin wave is therefore an interface mode.

In copper, the probability for low-energy excitations is less since the  $3d$  band is fully occupied. One therefore expects a larger mean-free path of electrons for electron energies below the plasmon energy. Thus, electrons of 6 eV energy in vacuum should be able to “look” through thicker capping layers. That is indeed the case. Figure 3 shows a series of spin wave spectra as a function of  $\Delta K_{\parallel}$  after deposition of 6 ML of Cu. The specific intensity of the spin wave loss at  $\Delta K_{\parallel} = 0.6$  Å<sup>-1</sup> and

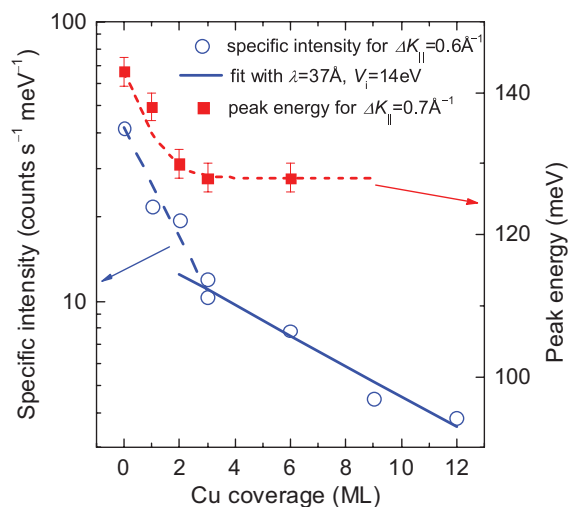


FIG. 4. (Color online) Specific intensity and peak energy of the spin wave loss at  $\Delta K_{\parallel} = 0.6$  and  $0.7$  Å<sup>-1</sup>, respectively, as a function of the thickness of the copper overlayer (see the text for discussion).

the peak energy as function of the thickness of the copper overlayer are shown in Fig. 4. As in the case of nickel, there is a sharp initial drop in intensity, followed by an exponential decrease. The decrease is, however, less steep than in the case of nickel. The analysis of the decay following Eqs. (2)–(4) yields a mean-free path of  $\lambda = 37$  Å. As in the case of nickel, the interface formation causes a reduction in the spin wave peak energy (Fig. 4).

Figure 5 shows the peak positions of the Ni/Co interface spin waves for wave vectors along the  $\langle 110 \rangle$  ( $\bar{\Gamma}\bar{X}$ ) direction with several sets of data for capping layers of 1, 1.5, and

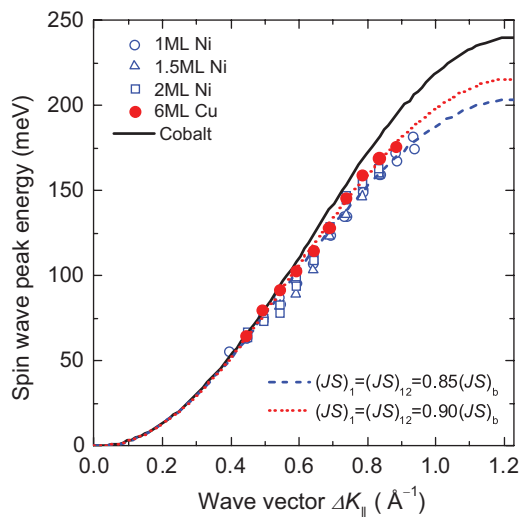


FIG. 5. (Color online) Peak energy vs wave vector transfer  $\Delta K_{\parallel}$  along the  $\langle 110 \rangle$  direction for the interface spin waves of the Ni/Co interface with 1, 1.5, and 2 ML Ni capping (circles, triangles, and squares, respectively) and for a capping with 6 ML Cu (solid red circles). The solid black line is the dispersion of the bare cobalt film. The blue dashed line and the red dashed line are fits to the Heisenberg model with modified coupling constants at the interface (see the text for discussion).

2 ML thickness depicted as circles, triangles, and squares, respectively. The data for a 6 ML capping with Cu are shown as red solid circles. The solid line in Fig. 5 depicts the dispersion of the bare cobalt surface, here represented by the result of the nearest-neighbor Heisenberg model with  $JS = 15$  meV which provides an excellent fit to the experimental data.<sup>5,26</sup> The data points for the interface modes systematically fall below that line. The difference is larger, the larger the wave vector is. On the other hand, there is no systematic deviation in the data for the three different Ni coverages. This shows that concerning the spin wave dispersion, the interface between Ni and Co is complete with a single Ni layer (see also Fig. 2). We attribute this fact to the strong localization of the partly occupied  $d$  electrons responsible for the intermetallic bonding as well as for the magnetic properties of the interface. Copper, on the other hand, has only delocalized  $sp$  electrons at the Fermi level.<sup>33</sup> It seems therefore plausible that the cobalt interface spin waves continue to be affected by a second and third Cu capping layer (see Fig. 4).

While it is understood that the Heisenberg model is not a suitable base for a theoretical description of spin excitations in  $3d$  metal systems,<sup>13,18–20,22</sup> it nevertheless serves as an interpolation scheme and may provide some hints to the origin of the frequency shift observed here. The deviation of the dispersion for the interface modes from the modes of the bare cobalt surface is well described by the nearest-neighbor Heisenberg model for the 8 ML slab when the influence of the capping layer is modeled by a reduction in the exchange coupling between cobalt atoms at the interface. The dotted and dashed lines in Fig. 5 are calculated assuming that the intralayer coupling in the interface layer ( $JS$ )<sub>1</sub> and the coupling between the interface layer and the next layer underneath ( $JS$ )<sub>12</sub>

are reduced to 90% and 85% of the value of the bare cobalt film [ $(JS)_b = 15$  meV] for Cu and Ni capping, respectively. With all reservations, one must have to the application of the Heisenberg model for  $3d$  metals, the overall picture appears to be that the exchange coupling constants  $JS$  at the interface are reduced upon capping. This conclusion is corroborated by the observation that capping of 1.9 ML fcc cobalt on Cu(100) with copper causes a substantial reduction in the Curie temperature of the films.<sup>34,35</sup> On the other hand, experimental evidence<sup>36,37</sup> as well as a comprehensive theoretical study of fcc Co(100)/Ni(100) and the Co(100)/Cu(100) interface<sup>38</sup> show that the effect of the interface on the magnetic moments of Co is small. According to the latter work, the Co moment increases by about 2% at the Ni interface and decreases by 2% at the Cu interface. Since the fit of the Heisenberg model to the experimental data calls for a reduction of the coupling constant  $JS$  by 15% and 10% for Ni and Cu, respectively, the reduction is attributed to a reduction of the exchange constants rather than to a reduction in the magnetic moments.

We finally note that the energy widths of the spin wave signals systematically increase upon deposition of the capping layers. Qualitatively, this observation is consistent with the increased number of channels for spin-flip excitations provided by the capping layer. Details of these results will be presented in connection with a theoretical *ab initio* study.<sup>39</sup>

J.R. gratefully acknowledges the financial support from NRW Research School “Forschung mit Synchrotronstrahlung in den Nano- und Biowissenschaften.” The authors also thank S. Lounis for helpful comments and critical reading of the manuscript.

\*h.ibach@fz-juelich.de

<sup>1</sup>Y. Zhang, T.-H. Chuang, K. Zakeri, and J. Kirschner, *Phys. Rev. Lett.* **109**, 087203 (2012).

<sup>2</sup>K. Zakeri, Y. Zhang, T.-H. Chuang, and J. Kirschner, *Phys. Rev. Lett.* **108**, 197205 (2012).

<sup>3</sup>H. Ibach, D. Bruchmann, R. Vollmer, M. Etzkorn, P. S. A. Kumar, and J. Kirschner, *Rev. Sci. Instrum.* **74**, 4089 (2003).

<sup>4</sup>H. Ibach, J. Rajeswari, and C. M. Schneider, *Rev. Sci. Instrum.* **82**, 123904 (2011).

<sup>5</sup>R. Vollmer, M. Etzkorn, P. S. Anil Kumar, H. Ibach, and J. Kirschner, *Phys. Rev. Lett.* **91**, 147201 (2003).

<sup>6</sup>W. X. Tang, Y. Zhang, I. Tudosa, J. Prokop, M. Etzkorn, and J. Kirschner, *Phys. Rev. Lett.* **99**, 087202 (2007).

<sup>7</sup>J. Prokop, W. X. Tang, Y. Zhang, I. Tudosa, T. R. F. Peixoto, K. Zakeri, and J. Kirschner, *Phys. Rev. Lett.* **102**, 177206 (2009).

<sup>8</sup>K. Zakeri, Y. Zhang, J. Prokop, T.-H. Chuang, N. Sakr, W. X. Tang, and J. Kirschner, *Phys. Rev. Lett.* **104**, 137203 (2010).

<sup>9</sup>Y. Zhang, P. Buczek, L. Sandratskii, W. X. Tang, J. Prokop, I. Tudosa, T. R. F. Peixoto, K. Zakeri, and J. Kirschner, *Phys. Rev. B* **81**, 094438 (2010).

<sup>10</sup>Y. Zhang, P. A. Ignatiev, J. Prokop, I. Tudosa, T. R. F. Peixoto, W. X. Tang, K. Zakeri, V. S. Stepanyuk, and J. Kirschner, *Phys. Rev. Lett.* **106**, 127201 (2011).

<sup>11</sup>T.-H. Chuang, K. Zakeri, A. Ernst, L. M. Sandratskii, P. Buczek, Y. Zhang, H. J. Qin, W. Adeagbo, W. Hergert, and J. Kirschner, *Phys. Rev. Lett.* **109**, 207201 (2012).

<sup>12</sup>J. Rajeswari, H. Ibach, and C. M. Schneider, *Europhys. Lett.* **101**, 17003 (2013).

<sup>13</sup>S. Lounis, A. T. Costa, R. B. Muniz, and D. L. Mills, *Phys. Rev. B* **83**, 035109 (2011).

<sup>14</sup>P. Buczek, A. Ernst, and L. M. Sandratskii, *Phys. Rev. B* **84**, 174418 (2011).

<sup>15</sup>S. Lounis, A. T. Costa, R. B. Muniz, and D. L. Mills, *Phys. Rev. Lett.* **105**, 187205 (2010).

<sup>16</sup>A. T. Costa, R. B. Muniz, S. Lounis, A. B. Klautau, and D. L. Mills, *Phys. Rev. B* **82**, 014428 (2010).

<sup>17</sup>A. T. Costa, R. B. Muniz, J. X. Cao, R. Q. Wu, and D. L. Mills, *Phys. Rev. B* **78**, 054439 (2008).

<sup>18</sup>A. T. Costa, R. B. Muniz, and D. L. Mills, *Phys. Rev. B* **69**, 064413 (2004).

<sup>19</sup>A. T. Costa, R. B. Muniz, and D. L. Mills, *Phys. Rev. B* **70**, 054406 (2004).

<sup>20</sup>R. B. Muniz, A. T. Costa, and D. L. Mills, *J. Phys.: Condens. Matter* **15**, S495 (2003).

<sup>21</sup>A. T. Costa, R. B. Muniz, and D. L. Mills, *Phys. Rev. B* **68**, 224435 (2003).

- <sup>22</sup>R. B. Muniz and D. L. Mills, *Phys. Rev. B* **66**, 174417 (2002).
- <sup>23</sup>M. Plihal, D. L. Mills, and J. Kirschner, *Phys. Rev. Lett.* **82**, 2579 (1999).
- <sup>24</sup>H. Tang, M. Plihal, and D. Mills, *J. Magn. Magn. Mater.* **187**, 23 (1998).
- <sup>25</sup>M. Plihal and D. L. Mills, *Phys. Rev. B* **58**, 14407 (1998).
- <sup>26</sup>J. Rajeswari, H. Ibach, C. M. Schneider, A. T. Costa, D. L. R. Santos, and D. L. Mills, *Phys. Rev. B* **86**, 165436 (2012).
- <sup>27</sup>F. Meier, S. Lounis, J. Wiebe, L. Zhou, S. Heers, P. Mavropoulos, P. H. Dederichs, S. Blügel, and R. Wiesendanger, *Phys. Rev. B* **83**, 075407 (2011).
- <sup>28</sup>J. Rajeswari, Ph.D thesis, Universität Duisburg-Essen, 2013.
- <sup>29</sup>H. Ibach, *Physics of Surfaces and Interfaces* (Springer, Berlin, 2006).
- <sup>30</sup>H. Ibach and J. Rajeswari, *J. Electron Spectrosc. Relat. Phenom.* **185**, 61 (2012).
- <sup>31</sup>M. Etzkorn, Ph.D thesis, Martin-Luther University Halle-Wittenberg, 2005.
- <sup>32</sup>J. Hong and D. L. Mills, *Phys. Rev. B* **62**, 5589 (2000).
- <sup>33</sup>H. Eckardt, L. Fritsche, and J. Noffke, *J. Phys. F: Met. Phys.* **14**, 97 (1984).
- <sup>34</sup>P. Srivastava, F. Wilhelm, A. Ney, M. Farle, H. Wende, N. Haack, G. Ceballos, and K. Baberschke, *Phys. Rev. B* **58**, 5701 (1998).
- <sup>35</sup>F. Wilhelm, U. Bovensiepen, A. Scherz, P. Pouloupoulos, A. Ney, H. Wende, G. Ceballos, and K. Baberschke, *J. Magn. Magn. Mater.* **222**, 163 (2000).
- <sup>36</sup>M. Gottwald, S. Andrieu, F. Gimbert, E. Shipton, L. Calmels, C. Magen, E. Snoeck, M. Liberati, T. Hauet, E. Arenholz, S. Mangin, and E. E. Fullerton, *Phys. Rev. B* **86**, 014425 (2012).
- <sup>37</sup>C. Vaz, G. Lauhoff, J. Bland, S. Langridge, D. Bucknall, J. Penfold, J. Clarke, S. Halder, and B. Tanner, *J. Magn. Magn. Mater.* **313**, 89 (2007).
- <sup>38</sup>A. M. N. Niklasson, B. Johansson, and H. L. Skriver, *Phys. Rev. B* **59**, 6373 (1999).
- <sup>39</sup>S. Lounis, J. Rajeswari, and H. Ibach (unpublished).